Polymer Chemistry

PAPER

Block, random and palm-tree amphiphilic fluorinated copolymers: controlled synthesis, surface activity and use as dispersion polymerization stabilizers

David Alaimo,[a] Alexandre Beigbeder,[b] Philippe Dubois,[b] Guy Broze,[a] Christine Jérôme[a*] and Bruno Grignard[a]

A series of novel fluorinated amphiphilic stabilizers of different architectures (diblock, grafted, or palm tree copolymers) were successfully prepared by reversible addition-fragmentation chain transfer. The surfactant properties of these copolymers were first evidenced by measuring the interfacial tension at the H_2O/trifluorotoluene (TFT) interface, and the results were correlated to the stabilizing efficiency in the dispersion polymerization of 2-hydroxyethyl methacrylate (HEMA) in trifluorotoluene. The effect of the architecture and concentration of the stabilizer on the morphology, the size and the stability of the obtained polyHEMA particles morphology were investigated. Whatever the architecture of the stabilizer, conditions could be adapted to produce submicronic spherical poly(HEMA) particles with a diameter around 300 nm and a quite narrow size distribution.

Introduction

Suspension, emulsion and precipitation polymerization processes are techniques of choice for the industrial production of polymers by radical polymerization as it presents numerous advantages, such as tolerance to high solids contents, to water or impurities, and high monomer conversion can be obtained[1-3]. The interest in synthesizing polymers in dispersed media relies not only in the industrial viability of the process itself but also on the possibility to synthesize highly uniform particles of tunable size and morphology[1-3]. In contrast to emulsion polymerization, dispersion polymerization is characterized by initially homogeneous conditions, i.e. the monomer is fully soluble in the continuous phase[4]. During the polymerization, an insoluble polymer is formed and phase separation occurs to form particles in the presence of a stabilizer. In order to prevent the aggregation, the stabilizer must be carefully chosen by considering the nature of the continuous phase and the used monomer[4]. For radical dispersion polymerizations of polar monomers in apolar media, amphiphilic macromolecular surfactants have been successfully used to insure the stability of the formed colloidal dispersion by steric repulsion[5-9]. In this context, fluorinated copolymers have found increasing interest for dispersion polymerization in easily removable solvents such as fluorinated solvents or supercritical carbon dioxide ($scCO_2$)[5-26]. Indeed, beside their high thermal and chemical stability[27, 28], perfluorinated polymers are widely known for their good solubility in these media[27-31] These polymers are used in industry for the production of various surface functionalized materials providing water repellent properties to textiles, plastics, paper and metals. They also find applications in fields such as cosmetics, foams, lubricants, in graphic imaging, and antifogging[27-31]. Being soluble in $scCO_2$, perfluorinated polymers have found applications in dispersion polymerizations of many vinyl monomers such as methyl methacrylate[5-7, 9-12], acrylonitrile[8, 13], N-vinylpyrrolidinone[14-16], vinyl acetate[17], styrene[18, 19], 2-hydroxyethyl methacrylate[20-23] and other methacrylic esters[10, 24] in this medium.

Recently, Ford et al. reported on the effect of the hydrophilic / fluorinated ratio of tailor-made fluorinated diblock copolymers on the stabilizing efficiency in the dispersion polymerization in fluorinated solvents[25]. Actually, amphiphilic diblock copolymers based on 2-ethylhexyl methacrylate (EtHexMA) and 1H,1H-perfluorooctyl acrylate (FOA) or 1H,2H,2H-perfluorooctyl acrylate (THFOA) were used in the crosslinking dispersion polymerization of EtHexMA with chloromethylstyrene in perfluorobutyl ethyl ether (HFE-7200). By adjusting the length of each sequence and consequently by modifying the hydrophilic / fluorinated ratio of the diblock copolymers, stable colloidal dispersions composed of quite large particles with a diameter in the range of 0.4 μm to 1 μm could be obtained.

In the present paper, the synthesis of uniform submicron cross-linked poly(2-hydroxyethyl methacrylate) (PHEMA) particles in a fluorinated solvent is targeted. We particularly investigated the role of the macromolecular architecture of the tailor-made fluorophilic stabilizers used on the particles size, and size distribution and on the dispersion stability. Hence, random, diblock and palm tree copolymers of similar HFR (Hydrophilic / Fluorinated Ratio) and composed of hydrophilic poly(ethylene oxide) (PEO) and poly(1,1,2,2-tetrahydroperfluorodecyl acrylate) (PFDA) fluorophilic sequences have been synthesized. In order to get a good control of the composition and architecture of the three types of targeted stabilizers, controlled radical polymerization (CRP) was selected. Reversible Addition Fragmentation Transfer Chain (RAFT) polymerization is particularly interesting and proved to be applicable to a wide range of monomers[32] including fluorinated monomers targeting a high diversity of architectures. For example, the availability of functional transfer agents (CTA) able to control the

polymerization allows the preparation of macroCTA leading to block copolymers. In addition, the relatively low temperature of polymerization and absence of metallic residue are other benefits of the RAFT process. According to some pioneer research groups[20, 26, 33,34], we thus choose this polymerization technique for building the fluorinated stabilizers used in the present study.

The effect of the surfactant architecture on the water/trifluorotoluene (TFT) interfacial stabilization efficiency was measured by the pendant drop method. Based on these collected data, the efficiency of the surfactants to produce well-defined monodisperse sub-micronic polyHEMA particles has been tested and rationalized. This work reports for the first time, on a systematic study of the influence of the stabilizer architecture on the TFT/water interface and subsequently on the size and stability of sub-micronic polyHEMA particles produced in TFT.

Experimental section

Materials

1H,1H,2H,2H-heptadecafluorodecyl acrylate (FDA, Aldrich, 96%) and 2-hydroxyethyl methacrylate (HEMA, Aldrich, 96%) were distilled under reduced pressure in order to remove the inhibitor and degassed by bubbling of nitrogen. Poly(ethylene glycol) monomethyl ether (PEO, Fluka M_n= 2000 g/mol) and Poly(ethylene glycol) methyl ether acrylate (APEO, Aldrich M_n 454 g/mol) were used as received. α,α,α-trifluorotoluene (TFT, Aldrich, 99+%) was degassed by bubbling of nitrogen before use. 2,2'-azo-bis(2-methylpropionitrile) (AIBN, Fluka) and 1,1,2-trichlorotrifluoroethane, CFC 113, (Aldrich, 99,8%) were used as received. S-1-Dodecyl-S-(α,α'-dimethyl-α''-acetic acid)trithiocarbonate (RAFT initiator) was synthesized as detailed by Shea et al[35].

Characterizations.

^{1}H NMR spectra were recorded with a 400 MHz Brucker spectrometer. ^{1}H NMR spectra of all polymers and copolymers were recorded in a 50/50 (v/v) CFC 113/CDCl$_3$ mixture, with TMS as an internal reference. Size-exclusion chromatography (SEC) of PEO was carried out in THF (flow rate: 1 ml/min) at 45°C using a SDF S5200 autosampler liquid chromatograph equipped with SDF refractive index detector. Columns (HP PL gel 5 μm, 10^5, 10^4, 10^3, and 10^2 Å) were calibrated with poly(ethylene oxide) standards. The morphology of the poly(2-hydroxyethyl methacrylate) particles was observed by scanning electron microscopy (SEM; JEOL JSM 840-A) after metallization with Pt (30 nm) in order to estimate the particles size. The number-average diameter of the particles, D_n, was calculated by measuring the diameter of 100 particles by using an image analyser (Vistametrix, version 1.33.0) applied to SEM images following formula 1, where ni designates the number of particles of diameter Di.

$$D_n = \Sigma\, n_i D_i\, /\, \Sigma\, n_i \qquad \text{Formula 1}$$

The weight average diameter, D_w, was calculated from :

$$D_w = \Sigma\, n_i D_i^{\,4}\, /\, \Sigma\, n_i D_i^{\,3} \quad \text{Formula 2}$$

The polydispersity index (PDI) was given by :

$$\text{PDI} = D_w\, /\, D_n \qquad \text{Formula 3}$$

The interfacial (TFT/water) tension was measured at 20°C (293K) with a pendant drop tensiometer (drop shape analysis DSA 10 Mk2 (Krüss)) equipped with a thermostated chamber and a Circulator Thermo HAAKE DC 10. The size distribution of diluted TFT dispersions were estimated by Photon Correlation Spectroscopy (PCS) using a particle-size analyser (Delsa Nano C, Particle Analyzer, Beckman Coulter) at 25°C. The intensity of scattered light was detected at 165° to an incident beam.

Synthesis of poly(ethylene oxide) macromolecular RAFT agent (PEO-CTA)

5 g of (α-methoxy, ω-hydroxy) poly(ethylene oxide) (2000 g/mol) are dried by three azeotrope cycles with toluene, then kept under dry inert atmosphere. In a dry round-bottomed flask of 100 ml, one introduces 1.82 g of RAFT agent (S-1-Dodecyl-S'-(α,α'-dimethyl-α''-acetic acid) trithiocarbonate) (0.005 mol: 2eq), 1.03 g of N,N' -dicyclohexylcarbodiimide (DCC) (0.005 mol: 2eq), 0.06 g of 4-(dimethylamino)pyridine (DMAP) (0.0005 mol: 0.2eq) and 40 ml of dry THF. This mixture is mixed about 10 minutes, and then added to the dry PEO using a thin stainless steel tube by nitrogen pressure. The resulting solution is mixed at ambient temperature during 120 h, then precipitated in diethyl ether and finally placed in cold room overnight. The precipitate is collected by filtration, and then dried under vacuum. The precipitation process was reiterated until a constant functionalization value was obtained. The recovered solid is analyzed by NMR ^{1}H and GPC and the functionalization yield is estimated at 99%.

Synthesis of PEO-*b*-PFDA via RAFT polymerization in presence of PEO-CTA

PEO-CTA (1.27 g, 0.537 mmol) was dissolved in 38 g of TFT (benzotrifluoride) in a 100 ml round-bottomed flask. The mixture was placed under inert atmosphere, then purged with nitrogen during 10 minutes in order to eliminate any trace from oxygen. In parallel, 0.0177 g of AIBN was dissolved in 2 g of TFT. This solution is transferred by difference of pressure in the tube containing the reaction mixture which is then placed at 80°C during 15 hours. Reaction crudes are regularly isolated and analyzed by NMR ^{1}H in order to determine conversion. Once a maximum conversion of 95% is reached, the copolymer is precipitated in methanol and recovered by filtration. The molecular weight of copolymer is determined by ^{1}H NMR analysis.

Synthesis of poly(heptadecafluorodecyl acrylate) (PFDA) via RAFT polymerization

FDA was polymerized under nitrogen. In a typical experiment, a glass tube was added with AIBN (0.0061 g, 3.75 10^{-5} mol) and S-1-Dodecyl-S-(α,α'-dimethyl-α''-acetic acid)trithiocarbonate (0.273 g, 7.5 10^{-4} mol), and the polymerization medium was degassed by three vacuum/nitrogen purge cycles. Then, 30 ml of TFT and 15 g of FDA (2.896 mmol) were added under nitrogen. Polymerization was carried out in an oil bath thermostated at 80°C. After 7 h, the conversion reach 90% and the polymer was three times precipitated in methanol, dried in vacuum at 40°C overnight, and characterized by ^{1}H NMR spectroscopy.

Synthesis of poly(heptadecafluorodecyl acrylate)-*b*-poly(polyethylene glycol methyl ether acrylate) diblock copolymers

In a typical experiment, PFDA (M_n = 18000 g/mol, 10 g, 5.55 10^{-4} mol), poly(ethylene glycol) acrylate (APEO) (Mn = 454 g/mol, 143 g, 3.15 mmol), and AIBN (0.005 g, 3 10^{-5} mol) were added into a glass tube and degassed by three vacuum/nitrogen cycles. TFT was then added under nitrogen and the reaction mixture was heated at 80°C for 4 h. The polymerization conversion was estimated to 96% and the copolymer was precipitated in methanol, dried in vacuum at 40°C for one night before being characterized by ^{1}H NMR spectroscopy.

Synthesis of Random copolymer of poly(ethylene glycol methyl ether acrylate) with 1H,1H,2H,2H-heptadecafluorodecyl acrylate

In a typical copolymerization experiment, the RAFT initiator (0.248 g, 6.82 10^{-4} mol) and AIBN (0.0056 g, 3.41 10^{-5} mol) and APEO (1.515 g, 3.34 10^{-3} mol) were added into a glass tube degassed by three vacuum/nitrogen cycles. Then, TFT (30 ml) and FDA (13,485 g, 2.603 10^{-2} mol) were added under nitrogen with a syringe. The mixture was heated at 80°C for 7 h until a conversation about 94% was obtained. The copolymer was repeatedly precipitated into methanol, dried at 40°C in vacuum overnight, and finally characterized by ^{1}H NMR spectroscopy.

Interfacial tension measurements (TFT/water)

TFT solutions of different copolymer concentrations were prepared with TFT previously saturated with doubly distilled water (mixing 24h). A drop of constant volume (10 μl) of each solution has been formed in water (8ml) and the dynamic interfacial tension γ(t) has been determined from the shape of the organic drop in water previously saturated with TFT. All the samples were let to equilibrate for a sufficient long time (minutes to hours) in order to reach constant readings, i.e. the equilibrium interfacial tension γ_{eq}. Data from at least three measurements were averaged for each concentration and displayed a maximum variation lower than 2%.

The Langmuir isotherm is commonly used to describe the interfacial absorption of surfactants[36]

$$\Gamma = \Gamma_{max} \; x \; c \; / \; (a_L + c)$$

Formula 4

Where Γ_{max} is the maximum amount of absorbed copolymer at saturation in mol/m² and a_L is the Langmuir constant, at which half the interface is covered by the surfactant. The variation of absorbed amount Γ on the surfactant concentration is expressed by the Gibbs absorption equation (formula 5)[36].

$$\Gamma = - 1/RT \; x \; d\gamma \, / \, d(ln \; c)$$

Formula 5

Where R is the gas constant, T is the absolute temperature, γ is the equilibrium interfacial tension, and c is the copolymer concentration (mol/l). The combination of formula 1 with formula 2 allows, after integration, to access Γ_{max} and a_L. The area occupied per molecule, A in nm², can be calculated by the formula 6[37].

$$A = 10^{18} / N_A \Gamma_{max}$$

Formula 6

Where N_A is the Avogadro constant.

Dispersion polymerization of 2-Hydroxyethyl methacrylate (HEMA) in α,α,α-trifluorotoluene (TFT)

In a typical experiment, a glass tube was added with AIBN (0.01 g, 6.09 10^{-5} mol) and PEO-*b*-PFDA (0.1 g, Mn = 21000 g/mol) and the polymerization medium was degassed by three vacuum/nitrogen purge cycles. Then, 10 ml of TFT, HEMA (1 g, 7.68 10^{-3} mol) and EGDMA (0.05 g, 2.52 10^{-4}) were added under nitrogen. Polymerization was carried out by immersing the reactor in an oil bath thermostated at 80°C, under stirring with a magnetic bar at 1000 rpm. After 2 h, the polymerization was stopped and the product characterized by scanning electron microscopy (SEM) and dynamic light scattering (DLS).

Results and discussion

Stabilizers synthesis

PEO-*b*-PFDA diblock copolymers, P(APEO-*co*-FDA) grafted copolymers and PFDA-*b*-PAPEO palm tree diblock copolymers were synthesized by RAFT (scheme 1) using a well suited carboxylic acid containing trithiocarbonate[35], i.e. (S-1-Dodecyl-S-(α,α'-dimethyl-α''-acetic acid)trithiocarbonate) as a control transfer agent (CTA) known for controlling the polymerization of styrene, acrylates, acrylonitrile, isoprene and acrylic acid. Moreover, our group and others demonstrated previously that the polymerization of a fluorinated acrylate, i.e. 1H,1H,2H,2H-heptacafluorodecyl acrylate[20, 26] was controlled by using this CTA.

Table 1 Macromolecular characteristics of the three copolymers exhibiting different architectures but keeping constant molecular weights and compositions.

no.	Copolymer	Mn PEO[a] (g/mol)	Mn PFDA[b] (g/mol)	HFR[e] (EO/FDA)	Mn Total (g/mol)
1	PEO$_{45}$-*b*-PFDA$_{37}$	2000[c]	19000[d]	1.2	21000
2	PFDA$_{35}$-*b*-PA(PEO$_9$)$_5$	2350[c]	18000[d]	1.3	20350
3	P(FDA$_{46}$-*co*-A(PEO$_9$)$_5$)	2100[c]	24000[d]	1.0	25100

[a] Experimental molecular weight of PEO calculated by ^{1}H NMR spectroscopy.
[b] Experimental molecular weight of PFDA calculated by ^{1}H NMR spectroscopy.
[c] For PEO-*b*-PFDA (**1**) : Mn of the hydrophilic segment of PEO. For P(FDA-*co*-APEO) (**3**) and PFDA-*b*-PAPEO (**2**): number of acrylic PEO monomer x Mn APEO, with Mn APEO = 454 g/mol.
[d] Number of acrylic fluorinated monomer x Mn FDA, with Mn FDA = 518 g/mol.
[e] Hydrophilic / Fluorinated Ratio (HFR) = number of ethylene oxide (EO) units / number of FDA units in the copolymers.

Polymer Chemistry

PAPER
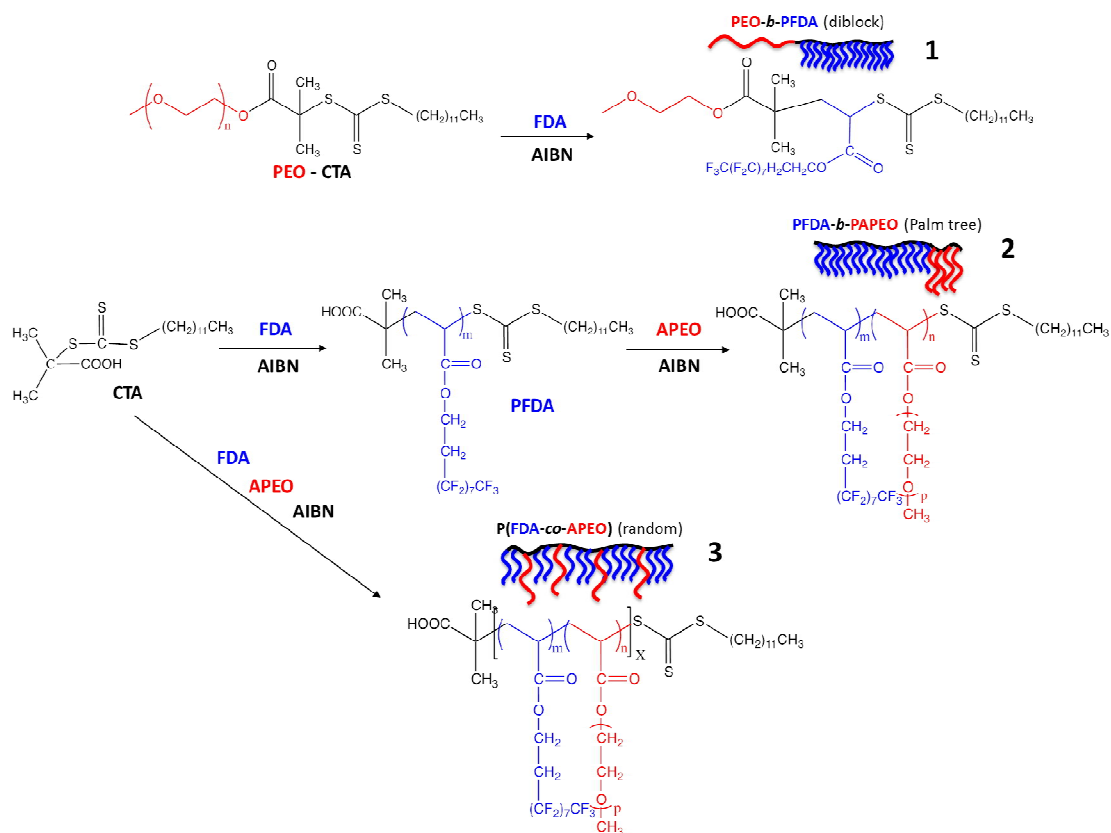
Scheme 1 Synthesis strategy of PEO-*b*-PFDA diblock copolymers (1) , PFDA-*b*-PAPEO palm tree diblock copolymers (2) and P(APEO-*co*-FDA) grafted copolymers (3) by controlled radical polymerization (RAFT).

1. Synthesis of PEO-b-FDA copolymers. In order to obtain an amphiphilic PEO-*b*-PFDA diblock copolymer having a lipophilic sequence of poly(1,1,2,2-tetrahydroperfluorodecyl acrylate) (PFDA) and hydrophilic sequence of poly(ethylene oxide), a macroRAFT agent of PEO was first prepared. A commercially available α-methoxy-ω-hydroxy-poly(ethylene oxide) of Mn = 2000 g/mol was reacted with S-1-dodecyl-S'-(α,α -dimethyl-α''-acetic acid) trithiocarbonate (CTA) at room temperature in the presence of dicyclohexylcarbodiimide (DCC) as desiccant agent and dimethylaminopyridine (DMAP) as catalyst ([CTA]/[DCC]/[OH] = 2/2/1). After 120h, CTA-modified PEO was purified by repeated precipitations in diethyl ether and after filtration and drying under vacuum until a constant functionalization yield was obtained. The solid was characterized by ^{1}H NMR spectroscopy.

The functionalization yield, higher than 99%, was estimated by ^{1}H NMR spectroscopy by comparing the relative intensity of resonances typical of the PEO end-groups, i.e. the α-methoxy group of PEO (CH₃O-, δ = 3,3 ppm) and the methyl group of the alkyl chain of the RAFT agent (CH₃, δ =0,87 ppm).

In a second step, the CTA-terminated PEO was used to initiate the FDA polymerization, in TFT at 80°C according to the strategy described by Lacroix-Desmazes et al.[20] (figure 1).

After 7h, the reaction was stopped and the FDA conversion, estimated by ^{1}H NMR spectroscopy by comparison of the relative intensity of resonances typical of the monomer (CH₂=CH-) at 6.05 ppm and the resonances corresponding to the methylene proton of the polyacrylate sequence (C(O)-O-CH₂) at 4.38 ppm, respectively, was higher than 95%. The experimental molecular weight of the PFDA sequence was estimated by ^{1}H NMR spectroscopy after purification of the polymer by precipitation in methanol and drying under vacuum. The molecular weight of the PFDA sequence (Table 1, entry 1) was determined by comparison of the relative intensities of the resonances characteristic of the repeating unit of PEO (CH₂-CH₂-O, 3.6 ppm) and the methylene protons of the PFDA block (C(O)-O-CH₂, 4.38 ppm) and was found close to the theoretical value.

2. Synthesis of PFDA-b-PAPEO palm tree diblock copolymers. In order to prepare the PFDA-*b*-PAPEO palm tree diblock

copolymers, the synthesis of PFDA macroinitiator of Mn = 18000 g/mol by RAFT using CTA was first performed in TFT at 80°C as reported elsewhere by some of us[38]. In a second step, the CTA end-capped PDFA chains were used to initiate the polymerization of PEO-based acrylate macromonomer.

By comparison of the resonances characteristic of the ω end-group of the PFDA chains (CH$_2$, δ = 3,4 ppm) and the resonance typical of the CH$_2$ of the repeating unit (CH$_2$, δ = 4.4 ppm), respectively, the experimental molecular weight of the PFDA sequence was estimated to 18000 g/mol which is consistent with the theoretical molecular weight and the monomer conversion (Table 1, entry 2)

In a second step, polymerization of polyethylene glycol methyl ether acrylate (APEO) was initiated by a PFDA of Mn = 18000 g/mol, leading to the PFDA-*b*-PAPEO palm tree copolymer (Figure 1). In order to preserve some coherence with the lypophilic/hydrophilic balance value of the PEO-*b*-PFDA diblock copolymers, the polymerization degree of the PAPEO was adjusted to 5 (Mn APEO = 454 g/mol).

In practice, the polymerization was conducted in TFT at 80°C. After 7h, the monomer conversion, calculated by comparing the relative intensity of resonances typical of the monomer (CH$_2$=C$\underline{H}$-) at 6.05 ppm and the protons of the methyl groups of the PAPEO chains (O-C$\underline{H_3}$) at 3,34 ppm, was estimated by ^{1}H NMR to 96%. After precipitation of the polymer in methanol and drying under vacuum, the experimental molecular weight of PAPEO sequence was determined by ^{1}H NMR on the basis of resonances characteristic of the CH$_3$ end-group of the PEO acrylate (O-CH$_3$, δ = 3,4 ppm) and the resonances of the methylene proton of the repeating unit of the PFDA sequence (CH$_2$, δ = 4.4 ppm), respectively (Figure 4). The obtained molecular weight (2350 g/mol) was found close to the theoretical value (Table 1, entry 2).

3. Synthesis of a P(APEO-co-FDA) random copolymer: A P(FDA-*co*-APEO) random copolymer was synthesized by copolymerizing FDA and APEO in TFT at 80°C in a statistical way in the presence of the RAFT CTA (figure 1). The FDA/APEO composition as well as the total molecular weight of the random copolymer, were calculated in order to keep coherent the lipophilic/hydrophobic balance value with the other copolymers architectures.

After 7h, the total monomer conversion was estimated to 94% by ^{1}H NMR by comparison of the relative intensity of resonances typical of the monomer (CH$_2$=C$\underline{H}$-) at 6.05 ppm and the CH$_2$ of the repeating unit (CH$_2$, δ = 4.4 ppm) of the polymer, respectively. After precipitation of the polymer in methanol and drying under vacuum, the experimental molecular weight as well as the composition of the copolymer were determined by ^{1}H NMR. The molecular composition of the copolymer was estimated by comparison of the relative intensities of the peaks characteristic of the methylene units of the FDA (C$\underline{H_2}$ of the FDA, δ = 4.4 ppm) and the CH$_3$ protons of the methoxy units of the APEO (O-C$\underline{H_3}$ of the APEO δ = 3.4 ppm).

The molecular weight of the polymer was estimated by comparison of the resonance characteristic of the CH group of the last monomer unit of the polymer chain (C$\underline{H}$-S-C(S)-S, δ = 4,95 ppm) and the repeating unit (C$\underline{H_2}$ of the FDA, δ = 4.4 ppm and the O-C$\underline{H_3}$ of the APEO δ = 3.4 ppm), respectively. We obtained molecular weights about 2100 g/mol for the PAPEO and

about 24000 g/mol for the PFDA, which were fitting the targeted molecular weights (Table 1, entry 3).

In order to attest for the random character of the RAFT polymerization of FDA and APEO, some samples were picked out the polymerization medium at regular intervals of time. As reported in Table 2, the FDA/APEO composition remains constant during the whole polymerization, in agreement with a random process.

Table 2 Macromolecular characteristics of P(FDA-*co*-APEO) sample during the polymerization.

Time (min)	Conversion[a]	Molar content[b] (APEO)	Molar content[c] (FDA)	Total molecular weight[d] (g/mol)
30	42 %	9.7 %	90.3 %	11000
60	70 %	9.5 %	90.5 %	18000
90	76 %	9.6 %	90.4 %	19000
120	82 %	9.7 %	90.3 %	20500
150	86 %	9.8 %	90.2 %	22000

[a] Monomer conversion estimated by ^{1}H NMR spectroscopy.
[b] Molar content of APEO in the copolymer calculated by ^{1}H NMR spectroscopy.
[c] Molar content of FDA in the copolymer calculated by ^{1}H NMR spectroscopy.
[d] Total molecular weight of PFDA-co-P(APEO) copolymer calculated by ^{1}H NMR spectroscopy.

Evaluation of tensioactive properties

The properties of the perfluorinated surfactants of different architecture but constant molecular weight and composition were evaluated by the method of the pendant drop. All the copolymers are soluble in TFT (a good solvent for both PFDA and PEO) but exhibit rather low solubility in water. The poor water solubility is expected with copolymers having a high fluorinated carbons content that are hydrophobic. As mentioned in Tables 1 and 3, the ratio between the number of ethylene oxide (EO) units and the number of fluorinated monomer (FDA) units was calculated based on the different polymerization degree for each copolymer. This Hydrophilic / Fluorinated Ratio (HFR) is used here to traduce the hydrophilic/fluorophilic balance of the three copolymers similarly to the more conventional hydrophilic/lipophilic balance (HLB) defined by Griffith[38-39] but for pegylated non fluorinated surfactants. As targeted, this HFR is approximately the same for the three copolymers which thus only differ from their architecture. Their tensioactive properties are thus expected to reflect essentially the copolymer topology. In practice, the interfacial measurements were performed by suspending in water (saturated beforehand with TFT), a TFT drop (saturated beforehand with water) containing the different surfactants at different concentrations. For each surfactant, a drop of constant volume of each solution (from 10^{-3} to 10^{-9} mol/l) was formed in water. The dynamic interfacial tension γ (mN/m) was determined from the shape of the TFT drop in water. The experiments were carried out until a constant reading is obtained (figure 1), corresponding to the interfacial tension at the equilibrium, γeq[40]. As a first observation, we can see that, for equal concentration, an important decrease of the dynamic tension for the block and palm tree stabilizer where the random

one shows a more flat profile. The rate of the decrease of the dynamic tension, decreases with time and was found to be dependent on the copolymer architecture and concentration (data not shown). As expected[41], at low stabilizer concentrations ($c < 10^{-7}$ mol/L) the equilibrium was not reached before several hours, time required to reach the TFT/water interface saturation by the amphiphilic copolymer. In contrast, for concentrations close to the saturation concentration (CS), i.e., the minimal concentration that leads to a maximal decrease of the interfacial tension, γ_{eq}, the steady-state of the interfacial tension (γ) was reached within a few minutes. For concentrations higher than CS, readings were constant after less than 1 hour.
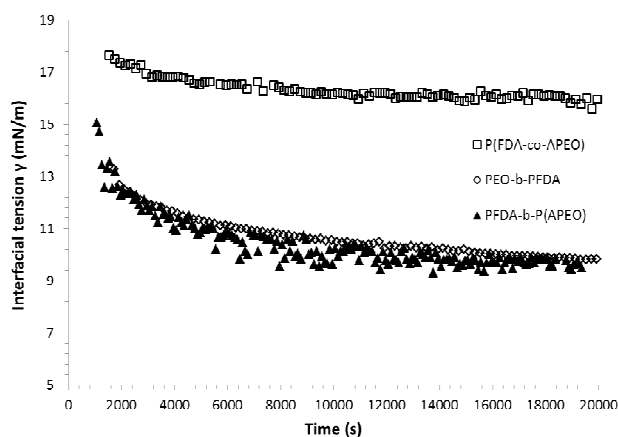
Figure 1 Evolution of dynamic interfacial tension γ (mN/m) according to time for the block (diamond), palm tree (triangle) and random (square) stabilizers at 10^{-5} mol/l.

The values of the obtained dynamic interfacial tension are then plotted according to the concentration for each type of copolymers (figure 2).
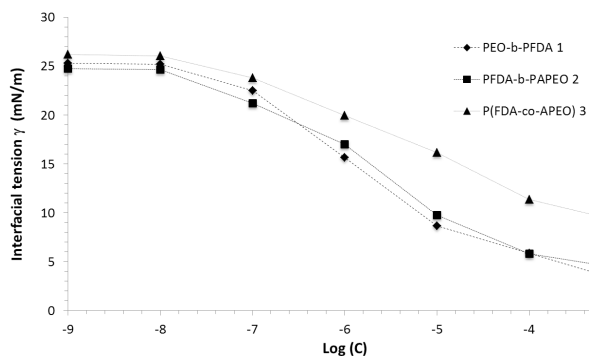
Figure 2 Interfacial tension at the equilibrium γ_{eq} (mN/m) versus copolymer concentration c (mol/l), at the TFT/water interface at 20°C. Curves fitted to formula 4 together with formula 5 (Gibbs equation).

For all the copolymers, these semi-logarithmic curves show a sigmoidal profile typical for interfacial stabilization with a significantly higher decrease for the diblock and the palm tree copolymers.

The shape of the curves in the low concentration domain is similar to the one obtained at the water-solvent surface with conventional surfactants: the steepness of the slope increases progressively as the logarithm of the concentration increases; however, at higher concentration, the steepness of the slope decreases only progressively, without really reaching an equilibrium value, when micelle formation occurs.

The shape of the interfacial tension – surfactant concentration isotherm at higher concentration could be explained by assuming the solubilisation of the surfactant in the TFT phase. This is not unrealistic as the hydrophobicity of the different copolymers is very high. This would mean that above a given concentration, there is a mass transfer of copolymer in the TFT phase, which implies that the actual copolymer concentration in the aqueous phase is significantly reduced. The critical saturation concentration, CS, was graphically determined at the intersection of the tangents to the sigmoidal plot. The saturation concentration (CS), the saturation absorption (Γ_{max}), the langmuir constant (a_L) and the area occupied per molecule (A) are reported in Table 3.

More quantitatively, the interfacial activity of copolymers can be expressed by the maximal decrease of the interfacial tension $\Delta\gamma$ (table 3). It was observed that the value of $\Delta\gamma$ was significantly higher for the diblock and palm tree copolymers compared to the random. Indeed, the curves of the diblock copolymers (PEO-*b*-PFDA and PFDA-*b*-PAPEO) have a relatively similar layout at all the range of concentrations and a very similar C_S, whereas the random copolymer with more raised C_S, exhibits the lowest surface activity. However, we note that the three types of architectures, at sufficiently high concentration, decrease the dynamic interfacial tension significantly. Another interesting data obtained using these isotherms reside in the area occupied per molecule at the interface for these three copolymers. It was concluded that the surface occupied by the random copolymer is slightly higher than that occupied by the diblock and palm tree copolymers. These observations might be related to the conformation that the polymer chains adopt at the interface. After diffusion of the copolymer to the interface, both segments (PEO and PFDA) must adopt the most energetically favourable conformation. The palm tree and diblock copolymers showed a hydrophobic segment of PFDA which is soluble in TFT and the hydrophilic segment of PEO being soluble in water. Therefore, both segments have probably a coil conformation in each phase rather than lying flat at the interface as observed for the random copolymer (figure 3). This hypothesis can explain the differences found between the diblock, and palm tree on one hand and the random copolymer on the other hand. Indeed, the diblock and palm tree copolymers showed an area occupied per molecule around 1,4 nm^2 whereas the random one occupies a surface around 2 nm^2. It can be easily understood that, for the same molecular weight and compositions, the random copolymer, with a lying flat conformation occupies a largest surface at the interface than the two other copolymers.

Table 3 Macromolecular copolymer characteristics of PEO-b-PFDA, PFDA-*b*-PAPEO and P(FDA-*co*-APEO) and interfacial properties.

no.	Copolymer	Architecture	HFR[a]	$\Delta\gamma$[b] (mN/m)	C_S[c] (mol/l)	Γ_{max}[d] (mol/m^2)	a_L[e] (mol/l)	A[f] (nm^2)
1	PEO$_{45}$-*b*-PFDA$_{37}$	Diblock	1.2	22	1.33 10^{-5}	1.39 10^{-6}	7.1 10^{-8}	1.19
2	PFDA$_{35}$-*b*-PA(PEO$_9$)$_5$	Palm tree	1.3	20.5	1.36 10^{-5}	1.22 10^{-6}	6.4 10^{-8}	1.36
3	P(FDA$_{46}$-*co*-A(PEO$_9$)$_5$	Random	1.0	17	1.71 10^{-5}	8.33 10^{-7}	7.7 10^{-8}	1.99

[a] Hydrophilic / Fluorinated Ratio (HFR) = EO units / FDA units in the copolymers.
[b] $\Delta\gamma = \gamma_0 - \gamma_f$, whereas γ_0 is the interfacial tension at the interface of pure trifluorotoluene/water and γ_f in the resulting surface tension for the highest concentration of copolymer solution.
[c] C_S = « saturation concentration » was determined as the intersection of the tangents at High concentration of the sigmoïdal plot.
[d] Γ_{max} = saturation absorption.
[fe] a_L = Langmuir constant, representing the concentration at which half of the interfacial coverage is reached.
[f] A = area occupied per molecule.
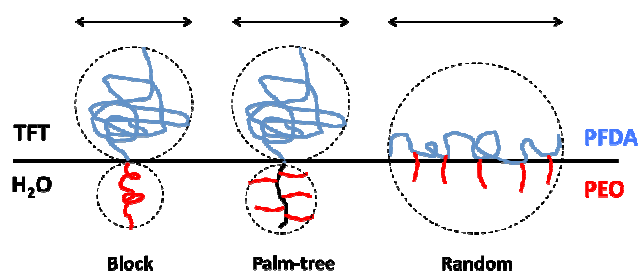
Figure 3 Absorption of PEO/PFDA copolymers at the TFT/H$_2$O interface

Dispersion polymerization of 2-Hydroxyethyl methacrylate (HEMA) in α,α,α-trifluorotoluene (TFT)

As the architecture of the stabilizer proved to have a significant influence on the surface activity, it should also influence the stabilization of dispersion polymerization. So, free-radical dispersion polymerization of HEMA was conducted in TFT in the presence of the different poly(1,1,2,2-tetrahydroperfluorodecyl acrylate)-based stabilizers. Using these stabilizers, it was hypothesized that the hydrophilic components of the copolymers (APEO) could act as effective anchoring groups to stabilize growing PHEMA particles[17] while the perfluorinated part highly soluble in TFT would avoid their aggregation. HEMA and the tree types of stabilizers (PEO-*b*-PFDA, P(FDA-*co*-APEO) and PFDA-*b*-PAPEO) are totally soluble in TFT whereas the resulting Poly(HEMA) is not. Optimization of the dispersion polymerization of HEMA was investigated by varying several parameters such as the architecture of stabilizers, the concentration of stabilizers (from 5 w/w % to 15 w/w % with respect to the monomer) and the monomer concentration (5 and 10 w/v % with respect to the dispersing solvent).

In practice, the monomer (HEMA), the surfactant, a cross-linking agent (ethylene glycol dimethacrylate, EGDMA) and AIBN were

dissolved in TFT at 80°C. After 2h, the HEMA conversion was higher than 90% and the polymerization medium was cloudy and formed of remarkably stable colloid dispersions with milky white appearance. The resulting polymer particles were characterized by scanning electron microscopy (SEM) and dynamic light scattering (DLS). In all cases, quite monodisperse spherical particles are obtained. Representative images of the collected particles with the different stabilizers are given Figure 4 a-c. The experimental conditions and the results relative to the various experiments are summarized in Table 4. For sake of comparison, polymerization of HEMA in the absence of stabilizer has been performed (table 4, entry 13) and leads to the formation of large aggregates of partially coalesced polymer particles with irregular shape that are characteristic of polymer obtained by precipitation polymerization under vigorous stirring (figure 4d).
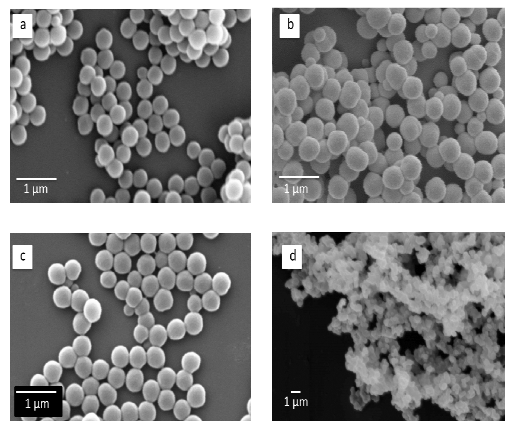
Figure 4 SEM images of PHEMA collected after polymerization in TFT in presence of a) block stabilizer (table 4, entry 2) b) palm tree stabilizer (Table 4 entry 6), c) random stabilizer (table 4 entry 10) d) without stabilizer (table 4 entry 13).

Table 4 : Experimental conditions and results for the dispersion polymerizations of HEMA in TFT.

Entry	Used copolymer	Architecture of the Stabilizer	Monomer concentration (w/v % versus TFT)	Stabilizer concentration (w/w % versus HEMA)	D_n[a] (nm) SEM	D_n[b] (nm) DLS	*PDI*[c]
1	PEO-*b*-PFDA	Diblock	10	5	559	849	1.08
2	PEO-*b*-PFDA	Diblock	10	10	463	473	1.11
3	PEO-*b*-PFDA	Diblock	10	15	391	458	1.35[e]
4	PEO-*b*-PFDA	Diblock	5	10	436	489	1.12
5	PFDA-*b*-PAPEO	Palm tree	10	5	479	690	1.07
6	PFDA-*b*-PAPEO	Palm tree	10	10	413	470	1.12
7	PFDA-*b*-PAPEO	Palm tree	10	15	404	460	1.42[e]
8	PFDA-*b*-PAPEO	Palm tree	5	10	418	458	1.18
9	P(FDA-*co*-APEO)	Random	10	5	790	800	1.09
10	P(FDA-*co*-APEO)	Random	10	10	570	589	1.15
11	P(FDA-*co*-APEO)	Random	10	15	515	530	1.34[e]
12	P(FDA-*co*-APEO)	Random	5	10	301	236	1.15
13[d]	/	/	10	0	/	/	Irregular[f]

Conditions : AIBN 1 w/w% (versus HEMA), T= 80°C, stirring rate = 1000 rpm, reaction time = 2h.
[a] D_n SEM = number average particle diameter determined by measuring the diameter of 100 particles using SEM images
[b] D_n DLS = number average particle diameter determined by dynamic light scattering (DLS).
[c] Polydispersity index (PDI) calculated by formula 3 from SEM data
[d] Precipitation polymerization in absence of stabilizer under vigorous stirring
[e] Bimodal distribution
[f] Large aggregates of partially coalesced and slightly cross-linked polymer particles, with irregular shape and broad size distribution

As demonstrated by the SEM and DLS data collected in table 4, whatever the stabilizer architecture, submicronic particles with a size ranging from 0.3 to 0.8 µm and a quite narrow size distribution were formed. As a rule, by increasing the stabilizer concentration from 5 wt% to 15 wt% compared to the monomer, the average particle size measured by DLS decreased from 700-850 nm for lowest tested stabilizer concentration (5 wt %) to 450-530 nm at the highest concentration (15 wt %), which is consistent with the results reported in the litterature[5, 9, 20, 24, 25].

Another interesting observation emanate from the analysis of particles synthesized using increasing stabilizer concentration of same architecture. When the stabilizer concentration is increased, produced particles show a distinct formation of a second population of smaller particles as observed comparing figure 5a and 5b. The number of this second population increases in function of the increase of the stabilizer concentration. This phenomenon could be attributed to the excess of PEO/PFDA copolymer, which is able to stabilize a second crop of smaller particles[42].
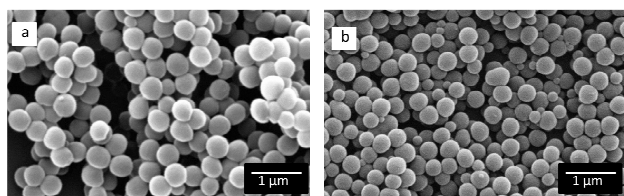
Figure 5 : Scanning electron microscopy (SEM) images of poly(HEMA) particles synthetized with a) 10 wt% and b) 15wt% (based on HEMA) of P(FDA-*co*-APEO).

Comparing now the particles size obtained with the different stabilizer architectures and for a monomer concentration of 10%, shows that the random copolymer gives at high concentration bigger particles (530nm) as compared to the block and palm tree stabilizers (480nm). Indeed, it was found that the decrease of the size of the PHEMA particles with the increase of the stabilizer concentration is much less pronounced with the surfactant of random architecture. As would suggest the figure 3 depicted from the tensiometric data, this observation could be due to a less efficient barrier to the particles growth with the random stabilizer lying flat on the particles surface as compared to a denser stabilizer layer with the block and palm tree copolymers. For an equal stabilizer concentration, the particles obtained with the random copolymer exhibit a larger diameter (about 20%) than the particles obtained with the block and palm tree stabilizers. According to the interfacial model showed in figure 3 and the tensiometric data summarized in table 3, as the particle surface coverage proved to be higher for the random one, a higher interface could in principle be stabilized with the random copolymer. This would lead to smaller particles, which is not what we observed. However, data reported in table 3 clearly show that the random copolymer is a weaker stabilizer ($\Delta\gamma$ = 17 mN/m) for the TFT / water interface as compared to the two other copolymers. So, even the random stabilizer is able to cover a larger surface than the other ones, it appears that the weaker stabilization efficiency cannot prevent particles growth e.g. by coalescence phenomena during polymerization. According to figure 3, the block and the palm tree stabilizers exhibit a thicker fluorinated layer at the interface than the random one, which is lying flat, and thus provide a much better protection against coalescence.

Moreover, if the initial monomer concentration appears to have only few impact on the particles size (compare entries 2-4 and 6-8 of table 4, respectively) in case of diblock and palm tree stabilizers, a strong reduction of the particles size (from 589 to 236nm) is observed when the monomer concentration is

decreased in presence of the random copolymer as surfactant (entries 10-12 of table 4). Still inspired by figure 3, the random copolymer occupying a larger surface area, and thus exhibiting a less dense packing on the particles would be able to stabilize a high number of particles that in case of low monomer concentration have a limited growth by starving conditions. This would thus limit the final particles size.

Finally, in order to confirm that optimum particles are obtained after 2h of reaction, we performed one experiment for a 24h period, using the P(FDA-*co*-APEO) stabilizer. No effect was observed by prolonging the reaction time except a slight increase of the polydispersity of the resulting particles (supporting information) with an average particle diameter almost unchanged. This comforts us in the choice of performing the reaction no longer than 2h.

Conclusions

Perfluorinated stabilizers of different architectures and controlled molecular weight and composition, i.e. random, block and palm-tree copolymers, were synthesized by the RAFT. The tensioactive behavior of each stabilizer was evaluated at the water/TFT interface by measurement of the interfacial tension. Strong dependence of the surface activity with the structure of the stabilizer was established. These results demonstrated that stabilizers with a blocky structure (diblock and palm-tree) exhibited stronger reduction of the interfacial tension than the random copolymer. These results also suggest different organization and packing density of the copolymer at the interface which was a strong incentive to compare these structures in a heterogeneous process like dispersion polymerization.

In the range of studied conditions for the free-radical dispersion polymerization of HEMA in TFT, small size and spherical PHEMA particles can be obtained for each type of stabilizers. Particles size can be adjusted by controlling the stabilizer concentration. Interestingly enough, the use of the random copolymer with a low monomer concentration allowed us to produce the smallest PHEMA particles of this study for which a mean diameter as low as 236nm has been observed.

Acknowledgements

Notes and references

a Center for Education and Research on Macromolecules (CERM), Chemistry Department, University of Liège (ULg), Sart-Tilman, Allée de la Chimie 3, Bat. B6a, B-4000 Liège, Belgium. Tel : (32)43663565, e-mail : d.alaimo@ulg.ac.be

b Laboratory of Polymeric and Composite Materials, Université de Mons-Hainaut, 20 Place du Parc, B-7000 Mons, Belgium.

† Electronic Supplementary Information (ESI) available: Particle size distribution histograms.

1. R. Arshady, *Colloid Polym Sci*, 1992, **270**, 717-732.
2. H.-H. Chu and E.-D. Ou, *Polymer Bulletin*, 2000, **44**, 337-344.
3. D. C. Blackley, *Emulsion Polymerization*, Wiley, New York, 1975.
4. K. E. J. Barret, *Dispersion Polymerization in Organic Media*, Wiley, London, 1975.
5. H. M. Woods, C. Nouvel, P. Licence, D. J. Irvine and S. M. Howdle, *Macromolecules*, 2005, **38**, 3271-3282.
6. M. R. Giles, R. M. T. Griffiths, A. Aguiar-Ricardo, M. M. C. G. Silva and S. M. Howdle, *Macromolecules*, 2000, **34**, 20-25.
7. C. Lepilleur and E. J. Beckman, *Macromolecules*, 1997, **30**, 745-756.
8. H. Shiho and J. M. DeSimone, *Macromolecules*, 2000, **33**, 1565-1569.
9. P. Christian, M. R. Giles, R. M. T. Griffiths, D. J. Irvine, R. C. Major and S. M. Howdle, *Macromolecules*, 2000, **33**, 9222-9227.
10. W. Wang, M. R. Giles, D. Bratton, D. J. Irvine, S. P. Armes, J. V. W. Weaver and S. M. Howdle, *Polymer*, 2003, **44**, 3803-3809.
11. A. M. Gregory, K. J. Thurecht and S. M. Howdle, *Macromolecules (Washington, DC, U. S.)*, 2008, **41**, 1215-1222.
12. H. S. Hwang, W.-K. Lee, S.-S. Hong, S.-H. Jin and K. T. Lim, *J. Supercrit. Fluids*, 2007, **39**, 409-415.
13. Z. Wang, Y. J. Yang, Q. Dong, T. Liu and C. P. Hu, *Polymer*, 2006, **47**, 7670-7679.
14. T. Carson, J. Lizotte and J. M. Desimone, *Macromolecules*, 2000, **33**, 1917-1920.
15. T. Berger, B. McGhee, U. Scherf and W. Steffen, *Macromolecules*, 2000, **33**, 3505-3507.
16. A. Galia, A. Giaconia, V. Iaia and G. Filardo, *J. Polym. Sci., Part A: Polym. Chem.*, 2003, **42**, 173-185.
17. Y. Yang, Z. Wang, Y. Gao, T. Liu, C. Hu and Q. Dong, *J. Appl. Polym. Sci.*, 2006, **102**, 1146-1151.
18. N. Baran, S. Deniz, M. Akguen, I. N. Uzun and S. Dincer, *Eur. Polym. J.*, 2005, **41**, 1159-1167.
19. H. Shiho and J. M. Desimone, *J. Polym. Sci., Part A: Polym. Chem.*, 2000, **38**, 1146-1153.
20. Z. Ma and P. Lacroix-Desmazes, *Polymer*, 2004, **45**, 6789-6797.
21. H. Shiho and J. M. DeSimone, *J. Polym. Sci., Part A: Polym. Chem.*, 2000, **38**, 3783-3790.
22. K. S. Oh, W. Bae and H. Kim, *Eur. Polym. J.*, 2008, **44**, 415-425.
23. H. S. Ganapathy, H. S. Hwang, M. Y. Lee, Y. T. Jeong, Y.-S. Gal and K. T. Lim, *J. Mater. Sci.*, 2008, **43**, 2300-2306.
24. H. Shiho and J. M. DeSimone, *Macromolecules*, 2001, **34**, 1198-1203.
25. Y. Zhu and W. T. Ford, *Macromolecules (Washington, DC, U. S.)*, 2008, **41**, 6089-6093.
26. B. Grignard, C. Jerome, C. Calberg, C. Detrembleur and R. Jerome, *J. Polym. Sci., Part A: Polym. Chem.*, 2007, **45**, 1499-1506.
27. T. Imae, *Current Opinion in Colloid & Interface Science*, 2003, **8**, 307-314.
28. S. C. Sharma, D. P. Acharya, M. García-Roman, Y. Itami and H. Kunieda, *Colloids and Surfaces A: Physicochemical and Engineering Aspects*, 2006, **280**, 140-145.
29. I. J. Park, S.-B. Lee, C. K. Choi and K.-J. Kim, *Journal of Colloid and Interface Science*, 1996, **181**, 284-288.
30. E. Kissa, *Surfactant Sci. Ser.*, 2001, **97**, 1-615.
31. J.-F. Berret, D. Calvet, A. Collet and M. Viguier, *Curr. Opin. Colloid Interface Sci.*, 2003, **8**, 296-306.
32. G. Moad, E. Rizzardo and S. H. Thang, *Polymer*, 2008, **49**, 1079-1131.

33. J. Zhou, L. Zhang and J. Ma, *Chem. Eng. J. (Amsterdam, Neth.)*, 2013, **223**, 8-17.
34. M. Zong, K. J. Thurecht and S. M. Howdle, *Chem. Commun. (Cambridge, U. K.)*, 2008, 5942-5944.
35. J. T. Lai, D. Filla and R. Shea, *Macromolecules*, 2002, **35**, 6754-6756.
36. C. Nouvel, C. Frochot, V. Sadtler, P. Dubois, E. Dellacherie and J.-L. Six, *Macromolecules*, 2004, **37**, 4981-4988.
37. M. J. Rosen, *Surfactants and Interfacial Phenomena*, Wiley, 1978.
38. J. Rieger, P. Dubois, R. Jerome and C. Jerome, *Langmuir*, 2006, **22**, 7471-7479.
39. P. Becher and M. J. Schick, *Noionic Surfactants*, Marcel Dekker, New York, 1987.
40. J. Eastoe and J. S. Dalton, *Adv. Colloid Interface Sci.*, 2000, **85**, 103-144.
41. C. Wollenweber, A. V. Makievski, R. Miller and R. Daniels, *Colloids Surf., A*, 2000, **172**, 91-101.
42. Y.-L. Hsiao, E. E. Maury, J. M. DeSimone, S. Mawson and K. P. Johnston, *Macromolecules*, 1995, **28**, 8159-8166.

Polymer Chemistry Accepted Manuscript

Block, random and palm-tree amphiphilic fluorinated copolymers: controlled synthesis, surface activity and use as dispersion polymerization stabilizers

David Alaimo,[a] Alexandre Beigbeder,[b] Philippe Dubois,[b] Guy Broze,[a] Christine Jérôme[a*] and Bruno Grignard[a]

Graphical abstract
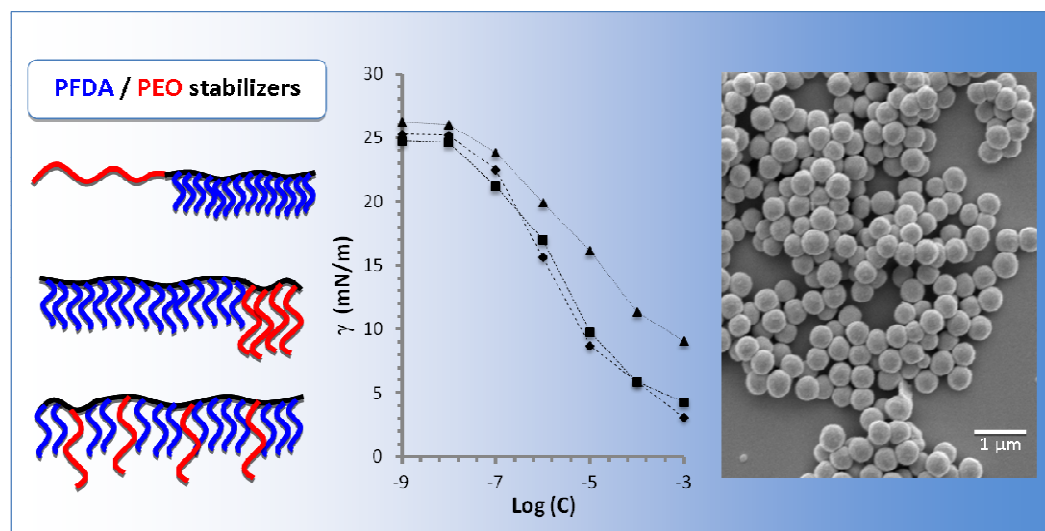
The architecture of the novel fluorinated copolymers drastically influence their stabilizing properties and ability to template particle formation